OPEN ACCESS

Quark–gluon plasma at the RHIC and the LHC: perfect fluid too perfect?

New Journal of Physics
The open-access journal for physics

Quark–gluon plasma at the RHIC and the LHC: perfect fluid too perfect?

James L Nagle[1,2,4], Ian G Bearden[2] and William A Zajc[3]

[1] Department of Physics, University of Colorado, Boulder, CO 80305, USA
[2] Niels Bohr Institute, Discovery Center, University of Copenhagen, Copenhagen, Denmark
[3] Department of Physics, Columbia University, New York City, NY 10027, USA
E-mail: jamie.nagle@colorado.edu

New Journal of Physics **13** (2011) 075004 (16pp)
Received 3 February 2011
Published 14 July 2011
Online at http://www.njp.org/
doi:10.1088/1367-2630/13/7/075004

Abstract. Relativistic heavy-ion collisions have reached energies that enable the creation of a novel state of matter termed the quark–gluon plasma. Many observables point to a picture of the medium as rapidly equilibrating and expanding as a nearly inviscid fluid. In this paper, we explore the evolution of experimental flow observables as a function of collision energy and attempt to reconcile the observed similarities across a broad energy regime in terms of the initial conditions and viscous hydrodynamics. If the initial spatial anisotropies for all collision energies from 39 GeV to 2.76 TeV are very similar, we find that viscous hydrodynamics might be consistent with the level of agreement for v_2 of unidentified hadrons as a function of p_T. However, we predict a strong collision energy dependence for the proton $v_2(p_T)$. The results presented in this paper highlight the need for more systematic studies and for a re-evaluation of previously reported sensitivities to the early time dynamics and properties of the medium.

[4] Author to whom any correspondence should be addressed.

Contents

1. Introduction

A physics case has been made that collisions at the Relativistic Heavy-Ion Collider (RHIC) produce a strongly coupled system that evolves as a nearly perfect fluid [1]; that is, the medium has a ratio of shear viscosity to entropy density η/s that is close to a conjectured minimum bound [2]. This categorization of the quark-gluon plasma as a nearly perfect fluid has opened up interesting connections to other strongly coupled systems in nature [3–5]. Many features of the RHIC experimental data are well described by theoretical calculations using the assumption of strong coupling. The most compelling of these results are fully relativistic viscous hydrodynamic calculations that describe the momentum anisotropy patterns measured by experiment. The initial overlap geometry in these nuclear collisions has a significant eccentricity for non-zero impact parameters. Both the general initial anisotropy and the event-by-event variations due to fluctuations in the nucleon positions can be described in terms of various moments $\epsilon_1, \epsilon_2, \epsilon_3, \epsilon_4, \epsilon_5, \ldots$ [6]. If the created medium were a non-interacting gas of particles, these spatial anisotropies would have no mechanism to translate into the momentum distributions of partons and eventually final state hadrons. However, in the limit of very strong interactions between the constituents (i.e. very short mean free paths), one expects substantial momentum anisotropies that might be describable via modeling based on viscous hydrodynamics. These momentum anisotropies are often described in terms of measured Fourier moments of the azimuthal distribution of particles—$v_1, v_2, v_3, v_4, v_5, \ldots$ [7]. Extensive measurements of the even moments of these observables by RHIC experiments indicate a strongly flowing fluid medium. Experimental efforts are now under way to study the odd Fourier flow coefficients that result from fluctuations, motivated by the important observations of [6, 8].

2. Energy dependence of perfection

The recently completed first Large Hadron Collider (LHC) heavy ion run at $\sqrt{s_{\mathrm{NN}}} = 2.76\,\mathrm{TeV}$ has provided an enormous increase in collision energy over the top RHIC center-of-mass energy of $\sqrt{s_{\mathrm{NN}}} = 200\,\mathrm{GeV}$. One of the more intriguing results is the measurement by the ALICE collaboration of the elliptic flow v_2 as a function of transverse momentum p_{T} for inclusive unidentified charged hadrons $(h^+ + h^-)$ [9], as shown in figures 1 and 2.

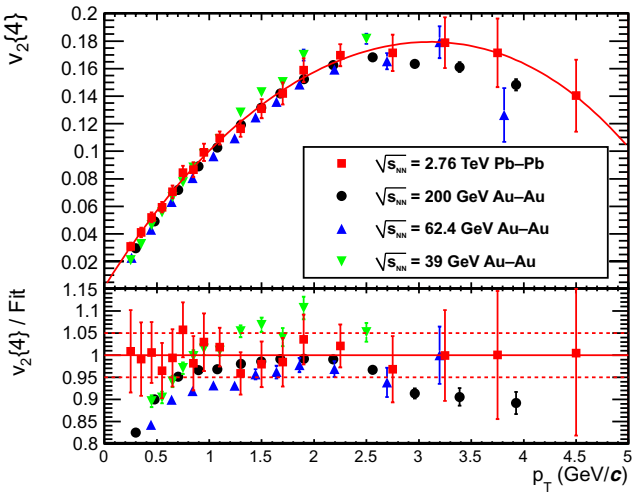

Figure 1. Experimentally measured $v_2\{4\}$ as a function of transverse momentum p_T for unidentified charged hadrons in the 20–30% centrality selection. Published results from the ALICE experiment at 2.76 TeV [9] and the STAR experiment at 200 GeV [11] are shown, along with preliminary results from lower energies [12]. The lower panel shows all data sets divided by a common fourth-order polynomial fit to the ALICE data points.

Comparing their measured $v_2\{4\}$ (a technique to measure v_2 via four-particle cumulants is given in [10]) with previous measurements at lower energies at RHIC [11, 12], striking agreement is seen. The optimal approach to quantifying the level of agreement between the values of $v_2(p_T)$ measured at LHC and RHIC would involve a full statistical and systematic uncertainty constraint fit using the methods developed in [13]. However, we note that by fitting a fourth-order polynomial to the published ALICE data, which include *only* statistical uncertainties, we obtain a $\chi^2/\text{d.o.f.} = 3.4/13$, corresponding to a p-value of 0.996; any inclusion of systematic errors would only decrease χ^2 and increase the p-value. The very low values of χ^2 result from the fourth-order cumulant method, which produces statistical correlations between the data points [14]. Additionally, other sources of systematic uncertainties are not fully quantified for either ALICE or STAR data sets. Nevertheless, as shown in the lower panel of figure 1 and right panels of figure 2, the agreement between the 2.76 TeV and 200 GeV data is at the level of a few per cent from $p_T = 0.5$–2.5 GeV, with larger deviations possible at lower and higher p_T. For the 20–30% centrality bin shown in figure 1, the agreement persists at the 5% level down to energies at least as low as 39 GeV.

The PHENIX experiment has published data for Au–Au collisions at $\sqrt{s_{NN}} = 200$ GeV on v_2 using the event plane method [15] that reveals similar agreement [16]. However, caution is needed regarding too fine a level of agreement or disagreement, because the methods have different sensitivities to flow fluctuations, which are appreciable at the 10–20% level in the final measured v_2 [17].

3. Perfect or too perfect

In this paper, we discuss some of the implications and new questions raised by this agreement between the v_2 measurements. In doing so, we consider the following scenario. Imagine that

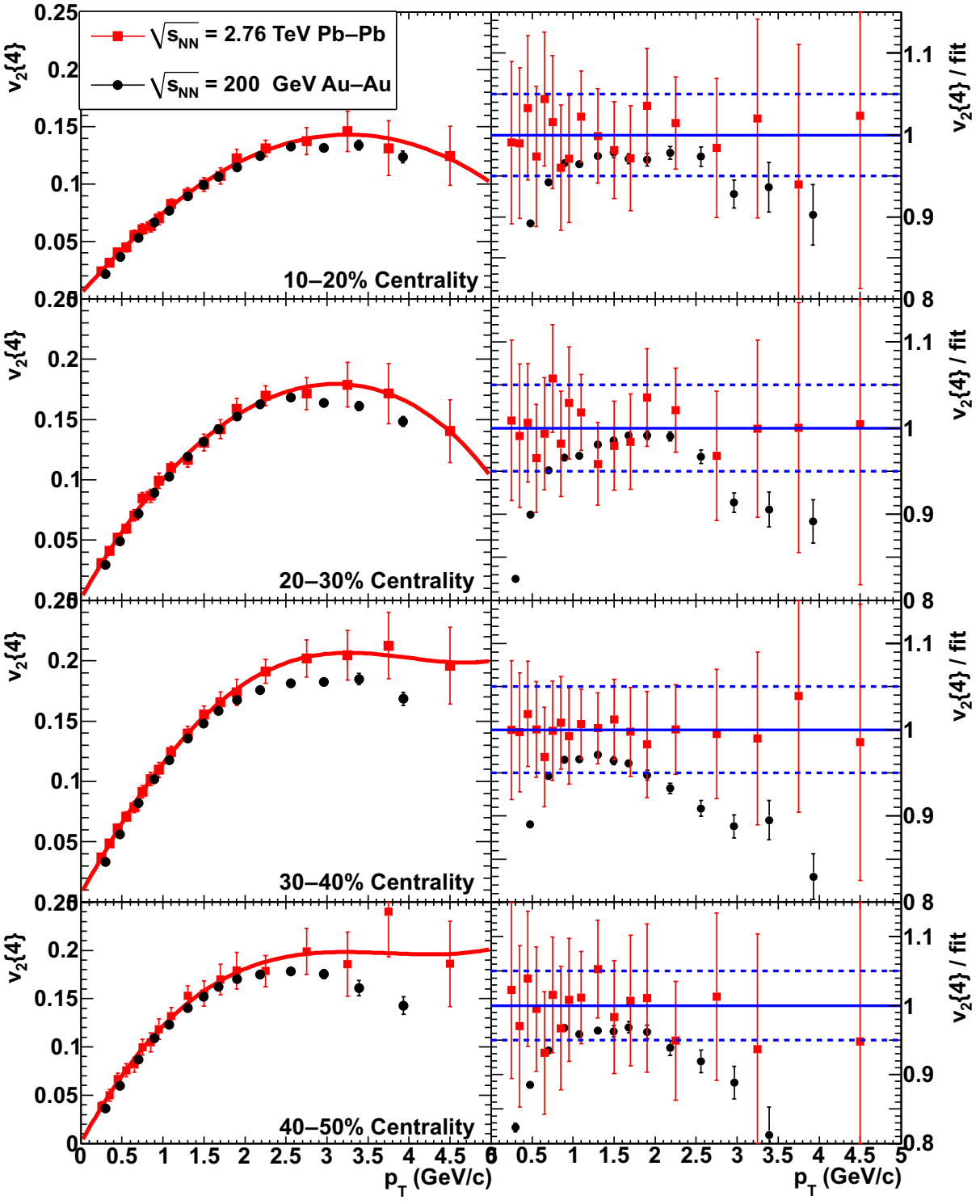

Figure 2. Experimentally measured $v_2\{4\}$ as a function of transverse momentum p_T for unidentified charged hadrons for centrality selections 10–20, 20–30, 30–40 and 40–50% from the top to the bottom. Published results from the ALICE experiment at 2.76 TeV [9] and the STAR experiment at 200 GeV [11] are shown. The right panels show the two data sets divided by a common fourth-order polynomial fit to the ALICE data points in each separate centrality selection.

we could prepare a system with a specific spatial distribution of energy density (in particular with a specific set of spatial anisotropies) and immediately evolve the system as a fluid with a specific fixed value for η/s to some appropriately large time. Let the medium have an equation of state (EOS) where the speed of sound is independent of temperature—for example, an ideal non-interacting gas with $\epsilon = p/3$. After the long evolution time, the system immediately breaks up into hadrons following the Cooper–Frye freeze-out prescription [18]. One might expect that the momentum anisotropy (e.g. v_2) as a function of p_T for hadrons would be the same regardless of the initial energy density scale. To be specific, if the central energy density were a factor of four higher, but the spatial distribution of that larger-energy density were identical, then despite larger pressure gradients in all outward directions, the *relative* pressure gradients in different directions would be the same. Thus, if one speculates that the fluid created at the RHIC is ideal ($\eta/s = 0$) or nearly ideal ($\eta/s = 1/4\pi$) and the same is true at the LHC, perhaps this explains the near-identical nature of the experimental data. A number of assumptions (some more justified than others) went into the above scenario. We examine some of these assumptions within the context of various models and speculate on what conclusions might be drawn. Useful reviews of recent work on viscous hydrodynamics can be found in [19–22].

First, we use the publicly available viscous hydrodynamic model of Romatschke and Luzum [23, 24] to test this simple scenario. We fix the initial conditions for Au–Au collisions with impact parameter $b = 7$ fm the using Monte Carlo Glauber results for binary collision positions [23]. We use an ideal gas EOS, $\eta/s = 0.001$ (not exactly zero for numerical stability reasons and known to reproduce the results of ideal hydrodynamical calculations), and an isothermal freeze-out temperature of 140 MeV, followed by Cooper–Frye hadronization and then resonance decays. We model two cases, one with an initial temperature of $T_i = 340$ MeV and the other with $T_i = 420$ MeV, as estimates for initial RHIC and LHC temperatures, respectively [25]. We use identical initial spatial distributions for both cases (with just a rescaling of the energy density for the appropriate initial temperature), to allow us to isolate the other dynamical effects.

The hydrodynamic results are shown in figure 3. As expected, the pions (and thus the unidentified hadrons, which are dominantly pions) have the same v_2 within a few per cent for $p_T > 1$ GeV. However, the proton $v_2(p_T)$ pattern appears to be shifted out in p_T for the higher initial temperature case. This is most likely due to the larger radial boost mapping onto the momentum distribution of protons (as detailed in [26]). One speculation is that the deviation at low p_T for pions, may be from resonance decay contributions. However, we have checked the primary (without decay contribution) v_2 for pions and similar differences between the two initial temperature cases are observed.

Secondly, we extend this question to the case of the QCD EOS (using the lattice QCD inspired EOS from [27]) and for $\eta/s = 0.001$. The left panel of figure 4 shows the results of this calculation again with two initial temperatures of 420 and 340 MeV. Despite the variation in the speed of sound c_s as a function of temperature due to the EOS, we find a similar qualitative result. For the range $p_T = 0.5$–3.5 GeV the pions, and therefore the unidentified charged hadrons, have the same v_2 within approximately 5%. It is worth noting that this v_2 signal is actually somewhat stronger for the lower $T_i = 340$ MeV. However, the proton $v_2(p_T)$ pattern again appears shifted out in p_T for the higher initial temperature case.

The right panel of figure 4 shows the results for the same QCD EOS but now with $\eta/s = 1/4\pi$. In this case, there is a noticeable difference at the highest p_T for all particles, with the lower-temperature case having a lower v_2. This observation suggests that even a minimal

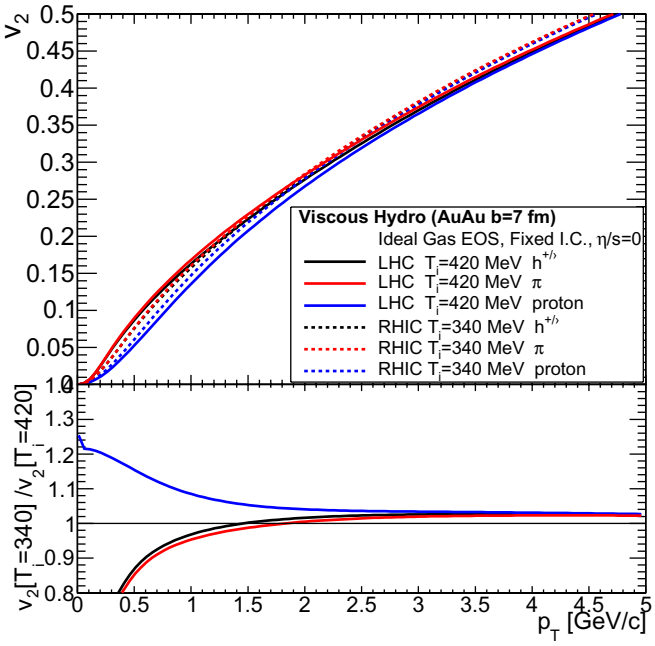

Figure 3. Viscous hydrodynamic results using an ideal gas EOS and $\eta/s = 0.001$. The v_2 for unidentified hadrons, pions and protons as a function of p_{T} are shown. The solid (dashed) lines are for $T_{\mathrm{i}} = 420(340)$ MeV, and the lower panel shows the ratio of v_2 values from the two cases.

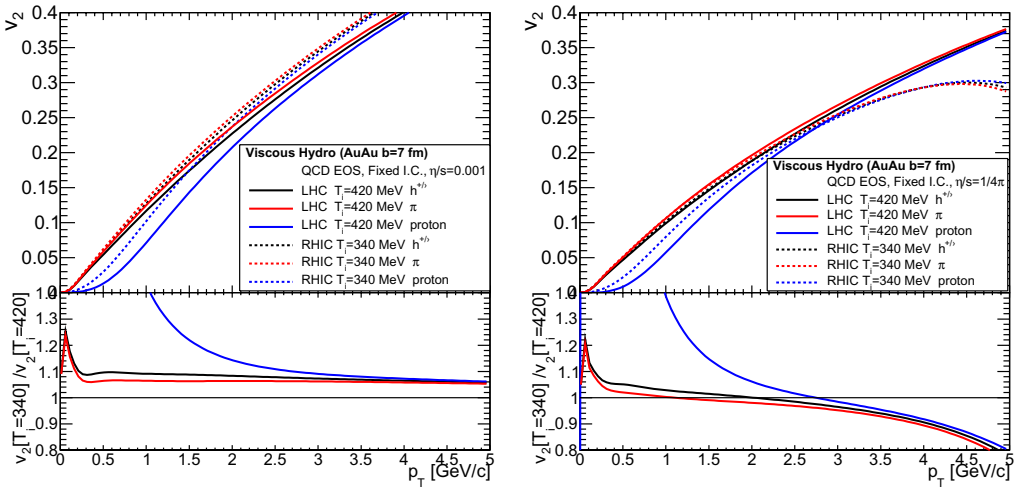

Figure 4. Viscous hydrodynamic results using an EOS determined from lattice QCD and $\eta/s = 0.001$ (left panel) and $\eta/s = 1/4\pi$ (right panel). The v_2 for unidentified hadrons, pions and protons as a function of p_{T} are shown. The solid (dashed) lines are for $T_{\mathrm{i}} = 420$ (340) MeV, and the lower panels show the ratio of v_2 values from the two cases.

viscosity plays a significant role in limiting the growth of v_2 with p_{T} for $p_{\mathrm{T}} > 3$ GeV at RHIC energies, while the significantly higher-energy densities at the LHC extend the regime where inertial forces dominate dissipation. We have run the $T_{\mathrm{i}} = 420$ MeV case to higher hadron p_{T}

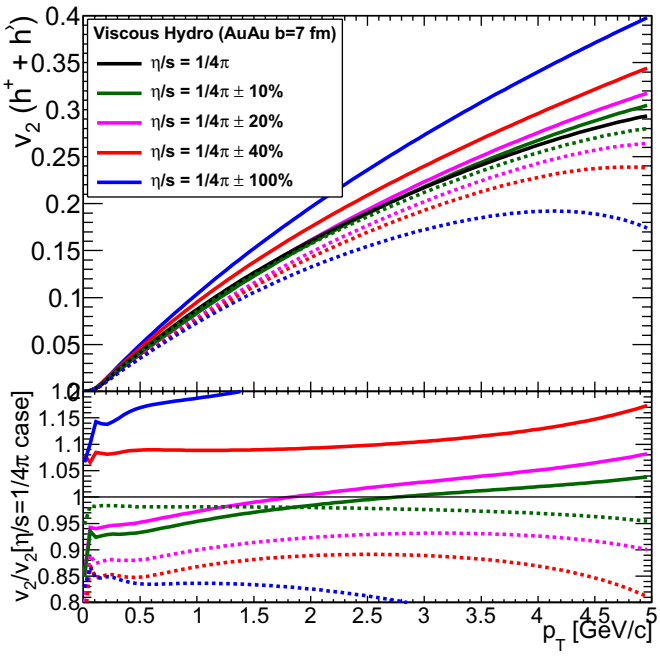

Figure 5. Viscous hydrodynamic results using QCD EOS for Au–Au $b = 7$ fm events, initial temperature $T = 340$ MeV and with varying η/s. The v_2 for unidentified charged hadrons as a function of p_T are shown. The black curve is for $\eta/s = 1/4\pi$. The other colors correspond to 10, 20, 40 and 100% change in η/s. The solid (dashed) lines correspond to a decrease (increase) in the ratio. The lower panel shows the ratio of all curves to the $1/4\pi$ case.

and find that the v_2 values do start to saturate for $p_T > 6.5$ GeV at a level near $v_2 \approx 0.44$. See section 4 for a discussion of other effects that must also be considered in this momentum regime. It is possible that a hint of this is seen in the experimental 200 GeV data in figure 2 in all centrality selections; but current uncertainties preclude any strong conclusion. Again, the proton v_2 pattern is shifted to higher p_T, leading to a rising ratio of the lower to the higher temperature case at $p_T < 2.0$ GeV. Thus, the measured v_2 for protons at the LHC is much anticipated.

Note that we have used smooth Glauber initial conditions for a fixed impact parameter $b = 7$ fm and no hadron re-scattering after freeze-out of the fluid in these calculations. Therefore, these quantitative calculations should not be compared directly with the experimental data, but rather reveal the qualitative trends with changing initial temperature.

4. Sensitivity to η/s

A crucial experimental question is the sensitivity of $v_2(p_T)$ to the value of η/s. A corresponding critical question for theory is the assumption employed by nearly all hydrodynamic calculations to date that η/s is independent of temperature. In this section, we examine these issues.

We have calculated the $v_2(p_T)$ for unidentified charged hadrons at RHIC temperatures with different variations in η/s as shown in figure 5. The black solid curve corresponds to $\eta/s = 1/4\pi$, the blue solid curve to $\eta/s \approx 0$ and the blue dashed curve to $\eta/s = 2/4\pi$. Note that we have not re-normalized the initial entropy density of the medium to maintain a fixed

final particle multiplicity or mean transverse momentum as done in other works;— see, for example, [28]. For 10% variation in η/s (green curves), there is very little change in the v_2 values (less than 5%). In fact, for these small 10–20% increases in η/s, v_2 shows a slight increase for p_T below $\sim$2 GeV.

It is clear that even a $\pm$40% change in η/s (red curves) results in only a 10% variation in v_2. Furthermore, it is important to note that this 10% variation is nearly independent of p_T from 0 to 5 GeV. Many comparisons of experimental data and viscous hydrodynamics focus on the differences at higher p_T because the theoretical calculations with different values of η/s *visually* split (as shown on a linear scale). However, this region in p_T is also sensitive to other effects such as the implementation of the departure $\delta f(p)$ from the equilibrium distribution $f_0(p)$ [29] and path-length-dependent jet energy loss (see, for example, [30]).

Given the relative insensitivity of $v_2(p_T)$ to the precise value of η/s, it is important to identify analysis procedures that maximize the sensitivity to this important quantity. Plotting the ratio of $v_2(p_T)$ from experimental measurements to that from theoretical calculations reveals important discriminating power at low p_T. It is at this low p_T that the experimental statistical uncertainties are smallest, and the systematic uncertainties (which require further attention to fully quantify them) are percentage uncertainties and thus are largely independent of p_T.

In most hydrodynamic calculations, the specific η/s value that is used is often referred to as an average. However, it is not simple to define what type of average this quantity is, as it is weighted in some complicated fashion over the space and time evolution. More realistically, it should be regarded as simply a fixed value used to obtain a first-order estimate. In this simple picture, the RHIC and LHC media would require values for η/s that differ significantly less than 40%.

We can examine the sensitivity to possible η/s variations with temperature by using a straightforward procedure. As a baseline, we have run with the QCD EOS and an initial temperature of 420 MeV and constant values for $\eta/s = 1/4\pi$ and also $\eta/s = 2/4\pi$. For comparison, we have implemented a simple step-function temperature dependence where for $T < 340$ MeV $\eta/s = 1/4\pi$ and for $T > 340$ MeV $\eta/s = 2 \times 1/4\pi$ (i.e. 100% larger). We also consider a second case where the step-function occurs near the transition temperature $T_c = 180$ MeV: that is, $\eta/s = 1/4\pi$ for $T < T_c$ and $\eta/s = 2 \times 1/4\pi$ for $T > T_c$. The results are shown in figure 6.

In the first case, the results show essentially no difference in $v_2(p_T)$ over the p_T range shown. The $T = 340$–420 MeV range is explored in the early times for the LHC-created medium and then after cooling we explore the same temperature range as that for the RHIC-created medium. Notably, there is no measurable difference in $v_2(p_T)$ for a factor of two change in the η/s ratio for the early time higher-temperature medium. Even if the step-function in the value of η/s occurs at the much lower temperature of $T_c = 180$ MeV, only a 10% decrease in v_2 at all p_T is seen. The modest value of these changes is striking and poses serious challenges to more precise extraction of transport coefficients via such measurements.

Recently, a study exploring a family of four temperature-dependent η/s cases was conducted [31], with a change in η/s at the transition temperature $T_c = 180$ MeV that includes a possible sharp rise in η/s just above the transition (for example, in the case labeled HQ the η/s value rises to $10 \times 1/4\pi$ at $T > 400$ MeV). While these very large values for η/s call into question the validity of the calculation in that parameter space [32], even in this extreme comparison, only a modest (less than 15%) change in the predicted v_2 is found at LHC energies (specifically the cases labeled LH–LQ to LW–HQ). Qualitatively this is consistent

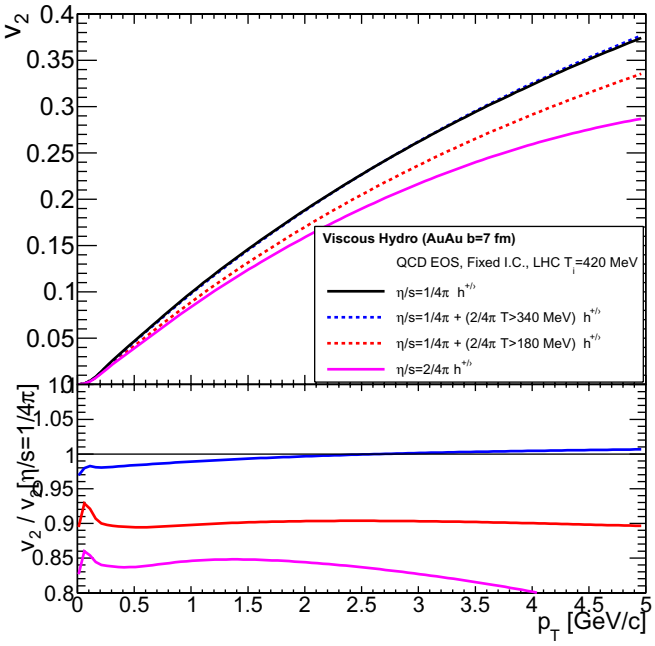

Figure 6. Viscous hydrodynamic results for v_2 versus p_T for unidentified charged hadrons using a QCD EOS and initial temperature $T = 420$ MeV. We compare the results with fixed $\eta/s = 1/4\pi$ and $\eta/s = 2/4\pi$ and two cases with a temperature-dependent value where $\eta/s = 1/4\pi$ at $T < 340$ MeV and $\eta/s = 2/4\pi$ at $T > 340$ MeV or $\eta/s = 2/4\pi$ at $T > 180$ MeV. The lower panel shows the ratio of all curves to the constant $\eta/s = 1/4\pi$ case.

with our finding where our very small (by comparison) factor of two change located at a higher temperature ($T > 340$ MeV) has very little impact. Thus, it appears *premature* to decide whether the higher-temperature region explored at the LHC (before cooling and evolving over the same temperature range as the RHIC) has the same or different η/s (as predicted in some models; see, for example, [33]). It is clear that more detailed studies of the temperature dependence are necessary; work in that direction is under way [28, 31]. A parallel critical area of research is recent work aiming at calculating these dynamical properties (for example, η/s as a function of temperature) for QCD on the lattice [34].

5. Initial conditions

In all of the above discussion, we have deliberately assumed that the initial spatial eccentricity and thermalization times do not vary between RHIC and LHC energies in order to separately study the effects due to η/s variations, the EOS and particle mass. Since ideal hydrodynamics predicts that v_2 should be proportional to the initial eccentricity, it is also important to investigate whether the initial spatial distribution at the LHC is the same as that at the RHIC. Another expected difference between these two energy regimes is in the equilibration time τ. It is often stated that the hydrodynamic matching to experimental data at the RHIC indicates rapid equilibration $\tau < 1.0$–$2.0\,\mathrm{fm\,c^{-1}}$. If in fact the final v_2 pattern is sensitive to the equilibration time, and the τ at LHC is significantly smaller than that at the RHIC, the near identity of the

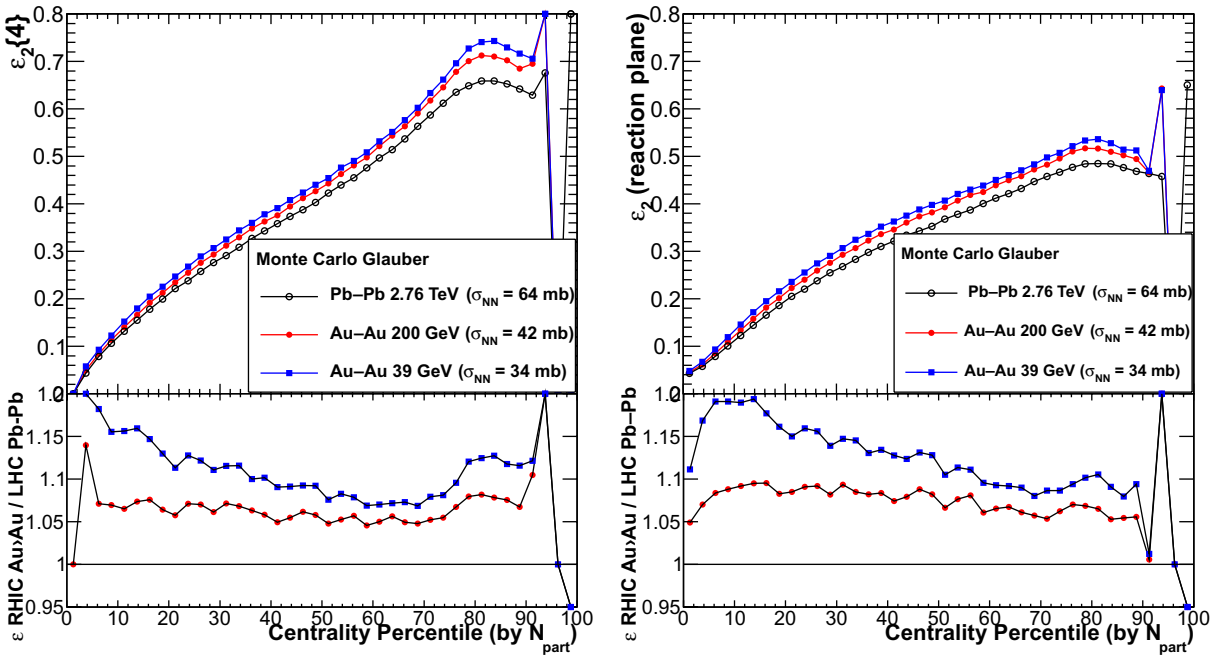

Figure 7. Monte Carlo Glauber results for Au–Au collisions at 39 and 200 GeV and Pb–Pb collisions at 2.76 TeV. The left panel shows $\epsilon_2\{4\}$ with respect to the reaction plane, and the right panel shows the rms ϵ_2 with respect to the participant plane, all as a function of collision centrality percentile (determined from the number of participating nucleons). The lower panels show the ratio of the RHIC to LHC eccentricity values.

$v_2(p_T)$ data from RHIC and LHC is deeply mysterious. Of course, one solution to this mystery is that the input assumptions are wrong, as discussed in [23], where it is argued that the purported sensitivity to rapid equilibration is incorrect.

In order to understand the potential range of variation in initial eccentricity, we have examined two of the currently used phenomenological models to calculate the initial spatial eccentricity. First, we use a Monte Carlo Glauber framework [35] to calculate the different eccentricities as a function of collision centrality percentile as determined by the number of participating nucleons (N_{part}). The most appropriate basis of comparison to compare data sets is the centrality percentiles (e.g. 20–30% of the total inelastic cross-section) being used by experiments; the eccentricity ratios show considerably higher variation if comparisons are made at a fixed participant number or impact parameter.

As already mentioned in section 1, there are multiple techniques for measuring v_2 that give results varying by of the order of 20%. These variations are due to the different influences of flow fluctuations and non-flow effects [17]. If we assume that initial eccentricities ϵ_n translate into momentum anisotropies v_n in individual events, then the most applicable for the $v_2\{4\}$ measurements is $\epsilon_2\{4\} = [2\langle\epsilon^2\rangle^2 - \langle\epsilon^4\rangle]^{1/4}$, which is shown in the left panel of figure 7. One observes an approximately 5% (10%) larger eccentricity for Au–Au at 200 (39) GeV collisions as compared with Pb–Pb collisions at 2.76 TeV. This 5% difference between 200 GeV and 2.76 TeV values was previously noted in [9].

There are three important contributors to these differences: firstly, the simple difference in atomic mass between Au (197) and Pb (208). Secondly, the nucleon–nucleon inelastic cross-sections are significantly increasing across the energy interval spanned by RHIC and LHC, ranging from 34 ± 3 mb at RHIC 39 GeV, 42 ± 2 mb at RHIC 200 GeV to 64 ± 5 mb at LHC 2.76 TeV (although this last value has not yet been experimentally finalized). A larger cross-section reduces the fluctuation in the number of participants, particularly in the periphery of the interaction zone, which in turn reduces the magnitude of $\epsilon_2\{4\}$, as seen in the left panel of figure 7. Thirdly, and related to the second, is that the larger total A–A inelastic cross section at the LHC changes the mapping of centrality percentile to the impact parameter range.

In the right panel, we show the ϵ_2 values with respect to the reaction plane. This shows a slightly larger 8% (15%) differences between 200 (39) GeV and 2.76 TeV. When comparing the corresponding values of ϵ_2 with respect to the reaction plane and $\epsilon_2\{4\}$, there is an increasing level of disagreement for more peripheral reactions, which is understood to result from non-Gaussian fluctuations that reflect the underlying Poisson fluctuations from discrete nucleons [35–37]. More central collisions quickly approach the limit of Gaussian fluctuations where the two estimates agree. However, for some hydrodynamic model calculations the role of (presumably real) fluctuations has been greatly reduced in spite of using Monte Carlo Glauber initial conditions by keeping the events fixed with respect to the reaction plane and *averaging* over many events to create smooth initial conditions as input. Note that this is exactly what is done for the hydrodynamic model comparisons in [38], where even for 40–50% central events this results in a 10% underestimate in the average eccentricity. The effect is even larger (more than a 25%underestimate) for the 70–80% centrality. Caution is therefore needed in making such comparisons with hydrodynamic models using this initialization and data. A useful discussion of this point is presented in [39] and may point to the need for running multiple hydrodynamic events on individually fluctuating initial conditions [40, 41].

We have also made similar comparisons for the color glass condensate (CGC) model-motivated initial condition calculation. This class of Monte Carlo calculations starts with the same Glauber model as that described above to determine the participants of a collision. However, a spatial region with say 20 participating nucleons is no longer assumed to produce 10 times the energy density as a region with two participating nucleons. This is due to the assumed saturation in the number of low-x gluons, whose wavefunctions overlap across the longitudinal extent of the nucleus. These calculations produce eccentricities that are larger than those from the pure Monte Carlo Glauber based on participating nucleons alone [42].

Here we utilize the rc-BK option [43] for the CGC initial conditions. Figure 8 shows $\epsilon_2\{4\}$ with respect to the participant plane as a function of centrality percentile for Au–Au at 39 and 200 GeV and for Pb–Pb at 2.76 TeV. One observes in the lower panel that the eccentricities agree within less than 2% for much of the centrality range (10–70%). At first this result seems counterintuitive since for higher collision energies, one should be probing lower-x gluons, saturation effects should increase and the eccentricity should increase relative to the Monte Carlo Glauber case. One does see a slight hint of this in that the Glauber difference between 200 GeV and 2.76 TeV shown in the left panel of figure 7 is 5% and in this case it is reduced to 2%.

In order to test this picture further, we have calculated the mean eccentricity with respect to the participant plane for Pb–Pb collisions for a large range of collision energies (17 GeV–200 TeV). Shown in the right panel of figure 8 are the resulting eccentricities for the rc-BK CGC case (solid lines) and the pure Monte Carlo Glauber (dashed lines) as a function of

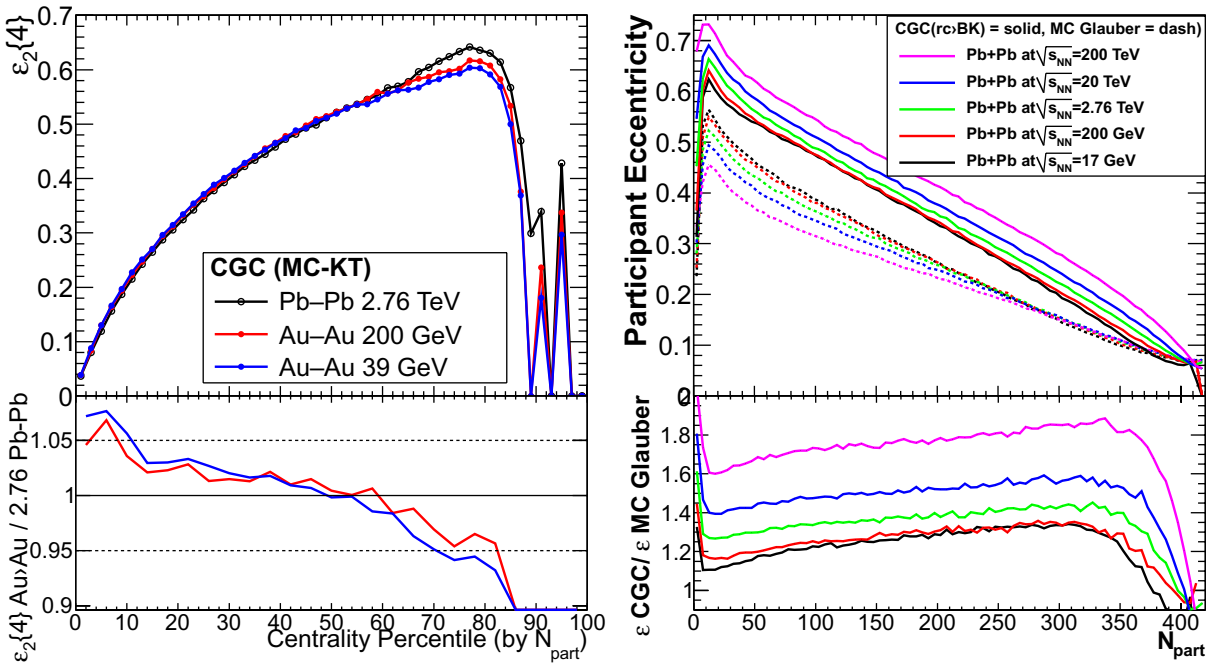

Figure 8. The left panel shows the rc-BK CGC calculation for $\epsilon_2\{4\}$ with respect to the participant plane for Au–Au at 39 and 200 GeV and for Pb–Pb at 2.76 TeV as a function of collision centrality percentile. The lower left panel shows the ratio of LHC to RHIC eccentricities. The right panel shows the CGC and Monte Carlo Glauber mean eccentricities for Pb–Pb collisions over a broad range of collision energies. The ratio of CGC eccentricities to those for the Monte Carlo Glauber is shown in the lower panel.

the number of participating nucleons. In the lower right panel, we calculate for each collision energy the ratio of CGC to Glauber eccentricity. As expected, the larger the collision energy, the larger the modification in the number of gluons and thus the larger the increase in eccentricity for the CGC case. However, the relative increase in eccentricity is only $\approx$10% from 200 GeV to 2.76 TeV. Curiously, this increase in eccentricity from saturation effects is largely canceled by the decrease in the underlying Monte Carlo Glauber eccentricity and in the mapping of centrality percentiles for Au–Au and Pb–Pb, as shown in the left panel. We note that different Monte Carlo Glauber implementations differ in how they smear the matter distribution corresponding to a single nucleon and whether they iteratively determine the Woods–Saxon parameters (as discussed in detail in [39]). For the comparison in figure 8, we utilize the same Monte Carlo Glauber as that set for initializing the CGC calculation.

One striking feature is that between 17 and 200 GeV the CGC-predicted $\sim$20% increase in eccentricity relative to the Monte Carlo Glauber changes only very slightly. In fact, the authors of the model note that for energies below 130 GeV the formalism breaks down since one is probing gluons with $x > 0.01$. This raises the interesting possibility that below some energy, there should be a transition in initial conditions from the larger CGC-calculated eccentricities to the lower Monte Carlo Glauber values. Data from the CERN-SPS heavy-ion fixed target program have not led to a definitive answer regarding v_2 at these energies due to different methods, centralities and varying baryon contributions to unidentified hadrons [44]. With

additional data from the RHIC energy scan, it will be very interesting to see how and whether the v_2 decreases as the center-of-mass is lowered (as predicted by many due to viscous effects in the hadronic re-scattering stage). The possible difference in initial eccentricity will require careful study (since CGC effects are not expected to play a role at these energies), and may be masked by other effects with a larger dynamics range, such as the (also poorly known) modifications to the EOS at finite baryon chemical potential.

6. Averages and Knudsen number method

The above discussion on the sensitivity to various parameters and their temperature dependence raises the question of whether simple models with a single η/s value, constant speed of sound and a single characteristic temperature can go beyond simple dimensionful scaling arguments to both capture the key physics and provide a basis for quantitative extraction of key dynamical parameters such as η/s. For example, it has been proposed that one can extract η/s from a fit to v_2 (integrated over all p_T) versus particle density using a simple scaling ansatz in the Knudsen number $K \equiv \lambda/\bar{R}$ [45] (here λ is the mean free path for momentum transport and $\bar{R}$ is a characteristic system size discussed below). Previously, we had investigated some of the underlying assumptions for this model and found important ambiguities in the parameterizations and sensitivities [46]. Despite these findings, the quantitative values from [45] are frequently quoted as reliable estimates for η/s.

It is of course possible to test this Knudsen scaling formalism by comparing it to the results from viscous hydrodynamic models where one knows the exact input η/s [47]. Those authors show that a Knudsen-based scaling of the results with η/s exists, but they did not check the formalism for self-consistency by using the same scaling [45] to compare the implied value of η/s to the input value used in the hydrodynamic calculations. We have done this using the exact procedure detailed in [46] whereby one arrives at a compact relation:

$$\frac{\eta}{s} = 0.32 K_0 T \bar{R} \left[\frac{(v_2/\epsilon)_{ih}}{(v_2/\epsilon)} - 1 \right], \tag{1}$$

where K_0 is a constant, T is the single constant temperature, $\bar{R} = 1/\sqrt{1/\langle x^2 \rangle + 1/\langle y^2 \rangle}$ is the characteristic scale for the strongest gradient in the initial matter configuration, and $(v_2/\epsilon)_{ih}$ is the ratio achieved in the ideal hydrodynamic limit.

Shown in figure 9 (left panel) are the results of viscous hydrodynamic calculations (using the model from [24]) cast in these quantities for three different fixed (centrality-independent) values of $\eta/s = 0.001, 1/4\pi$ and $2/4\pi$. The two finite viscosity cases are fitted using the Knudsen number formulation, and provide a reasonable fit to the theory points. We note that other parameterizations described in [46] give equally good fits. Then, utilizing the information on the initial conditions in the model for $\bar{R}$ and assuming a temperature $T = 200$ MeV (as was done in [45]), we extract the values of η/s as a function of centrality (shown in the right panel of figure 9).

It it is immediately clear that the extracted values for η/s are strongly centrality dependent, despite the fact that η/s was input as a constant for all centralities. While it has been postulated that this variation with centrality mimics viscous effects due to the finite lifetime of the system, this hypothesis then raises the question of why such a large early freeze-out effect would maintain the expected curvature relation for the approach to ideal hydrodynamics as a function of centrality. Even more importantly, the numerical value for the η/s extracted in central A–A

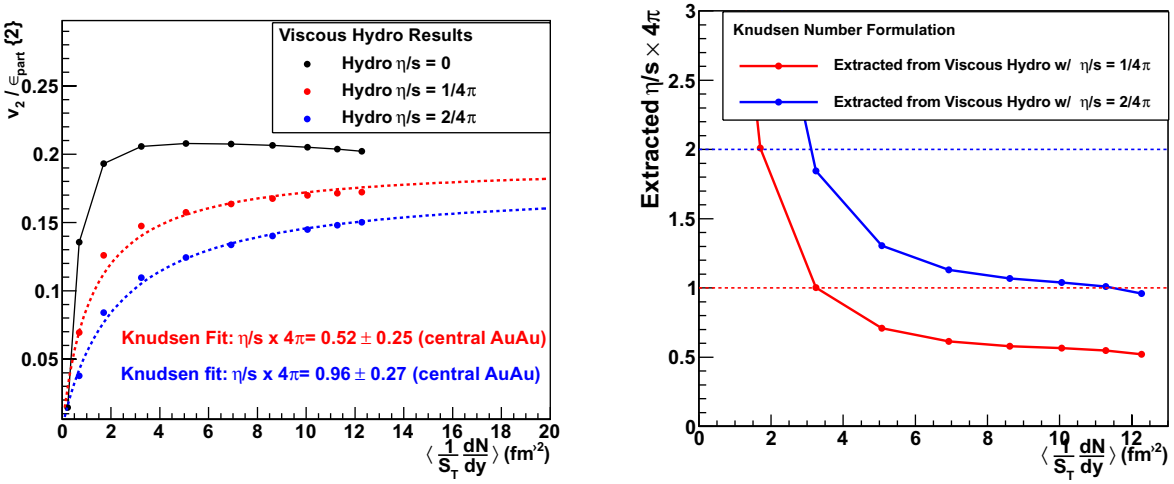

Figure 9. The left panel shows the results for $v_2/\epsilon_{\rm part}$ as a function of the transverse particle density $\langle 1/S_{\rm T}\, {\rm d}N/{\rm d}y\rangle$ from calculations of viscous hydrodynamics with fixed $\eta/s = 0.001$, $1/4\pi$ and $2/4\pi$. The red and blue curves are fits to the calculation using the Knudsen number formalism. The right panel shows the resulting Knudsen number extraction for η/s as a function of the same transverse particle density. The dashed lines represent the true η/s for the two cases as input to the viscous hydrodynamic model.

collisions is incorrect by a factor of two. Taken together, these observations argue strongly against simply 'calibrating' the procedure to remove the factor of two discrepancy. Any such renormalization should also be required to reproduce the input constancy of η/s, which in turn would require additional centrality-dependent adjustments to the parameters that appear in equation (1). Such an ad hoc procedure is clearly unsatisfactory, especially given the availability of the very hydrodynamic calculations that would be employed to reach a forced consistency. The inescapable conclusion is that the most reliable method currently available for the extraction of η/s from experimental data is direct comparison to the output of hydrodynamic calculations, keeping in mind the issues identified in the preceding sections of this paper. It should be noted that there are additional concerns not addressed here, in particular that of transport in the hadronic phase. However, it is understood that the larger mean free paths in the hadronic phase lead to larger viscosity, so that the correct interpretation of the values used in the hydrodynamic calculations that ignore transport after hadronization would be upper bounds for η/s.

7. Summary

In this paper, we have explored some of the various inputs regarding hydrodynamic modeling of heavy-ion collisions and the sensitivity of the final measured v_2 versus $p_{\rm T}$ to these inputs. This work was motivated by the striking agreement between v_2 measurements over a broad range of energies. Quantifying the precise level of agreement, and then in turn understanding the physics implications of the trends in the data, requires a detailed understanding of these sensitivities. Even at the initial stage in such a systematic exploration, the argument that the agreement is the result of fortuitous cancelation of effects should be viewed with great suspicion. As an example,

the agreement in the $v_2(p_T)$ data between RHIC and LHC is inconsistent with the predictions of the models [31], which assume significantly different transport regimes at these two energies. It will be most interesting to extend hydrodynamic calculations to compare with new data at the lower colliding energies, although issues of baryon contributions and modeling of the EOS will also need to be addressed. It is likely that these dynamic effects will greatly exceed the relatively modest variations in initial state eccentricity, which is not more than 10% when evaluated as a function of centrality rather than the number of participants.

We have also highlighted the need to take ratios that reveal that the greatest sensitivity to viscosity effects is at lower p_T where the data are also the most accurate. These results highlight the need for more systematic studies and a re-evaluation of previously reported sensitivities to the early time dynamics and properties of the medium. Similarly, comparisons of the data to ever more sophisticated hydrodynamic and transport calculations, rather than parameterizations with underlying dynamical assumptions unsupported by detailed examination, are far more likely to lead to precision extraction of transport coefficients. An important development in these investigations is the public availability of modern and reliable hydrodynamic codes, which greatly leverage the community's ability to pursue these exciting topics.

Acknowledgments

We acknowledge useful discussions with Javier Albacete, Adrian Dumitru, Kevin Dusling, Matthew Luzum, Michael McCumber, Jean-Yves Ollitrault, Paul Romatschke and Raimond Snellings. We particularly appreciate the public availability of these algorithms and experimental data. JLN acknowledges financial support from the US Department of Energy Division of Nuclear Physics (grant no. DE-FG02-00ER41152), the Discovery Center at the Niels Bohr Institute and the Nordea Foundation. IGB was supported by the Danish National Science Research Council and the Danish National Research Foundation. WAZ was supported by the US Department of Energy (grant no. DE-FG02-86ER40281).

References

[1] Adcox K *et al* [PHENIX Collaboration] 2005 *Nucl. Phys.* A **757** 184–283 (arXiv:nucl-ex/0410003)
[2] Son D T and Starinets A O 2007 *Ann. Rev. Nucl. Part. Sci.* **57** 95–118 (arXiv:0704.0240 [hep-th])
[3] Johnson C V and Steinberg P 2010 *Phys. Today* **63** 29–33
[4] Thomas J E 2010 *Phys. Today* **63** 34–7
[5] Jacak B and Steinberg P 2010 *Phys. Today* **63** 39–43
[6] Alver B and Roland G 2010 *Phys. Rev.* C **81** 054905 (arXiv:1003.0194 [nucl-th])
[7] Ollitrault J-Y 1992 *Phys. Rev.* D **46** 229–45
[8] Sorensen P 2010 *J. Phys. G: Nucl. Part. Phys.* **37** 094011 (arXiv:1002.4878 [nucl-ex])
[9] Aamodt K *et al* [The ALICE Collaboration] 2010 arXiv:1011.3914 [nucl-ex]
[10] Borghini N, Dinh P M and Ollitrault J-Y 2001 *Phys. Rev.* C **64** 054901 (arXiv:nucl-th/0105040)
[11] Abelev B I *et al* [STAR Collaboration] 2008 *Phys. Rev.* C **77** 054901 (arXiv:0801.3466 [nucl-ex])
[12] Kumar L [for the STAR Collaboration] 2011 arXiv:1101.4310 [nucl-ex]
[13] Adare A *et al* [PHENIX Collaboration] 2008 *Phys. Rev.* C **77** 064907 (arXiv:0801.1665 [nucl-ex])
[14] Snellings R 2011 private communication
[15] Adare A *et al* [PHENIX Collaboration] 2010 *Phys. Rev. Lett.* **105** 062301 (arXiv:1003.5586 [nucl-ex])
[16] Lacey R A *et al* 2010 arXiv:1011.6328 [nucl-ex]
[17] Ollitrault J-Y, Poskanzer A M and Voloshin S A 2009 *Phys. Rev.* C **80** 014904 (arXiv:0904.2315 [nucl-ex])

[18] Cooper F and Frye G 1974 *Phys. Rev.* D **10** 186
[19] Heinz U W 2009 arXiv:0901.4355 [nucl-th]
[20] Teaney D A 2009 arXiv:0905.2433 [nucl-th]
[21] Romatschke P 2010 *Int. J. Mod. Phys.* E **19** 1–53 (arXiv:0902.3663 [hep-ph])
[22] Hirano T, van der Kolk N and Bilandzic A 2010 *Lect. Notes Phys.* **785** 139–78 (arXiv:0808.2684 [nucl-th])
[23] Luzum M and Romatschke P 2008 *Phys. Rev.* C **78** 034915 (arXiv:0804.4015 [nucl-th])
[24] Romatschke P and Romatschke U 2007 *Phys. Rev. Lett.* **99** 172301 (arXiv:0706.1522 [nucl-th])
[25] Luzum M and Romatschke P 2009 *Phys. Rev. Lett.* **103** 262302 (arXiv:0901.4588 [nucl-th])
[26] Kestin G and Heinz U W 2009 *Eur. Phys. J.* C **61** 545–52 (arXiv:0806.4539 [nucl-th])
[27] Laine M and Schroder Y 2006 *Phys. Rev.* D **73** 085009 (arXiv:hep-ph/0603048)
[28] Shen C and Heinz U 2011 arXiv:1101.3703 [nucl-th]
[29] Dusling K, Moore G D and Teaney D 2010 *Phys. Rev.* C **81** 034907 (arXiv:0909.0754 [nucl-th])
[30] Jia J, Horowitz W A and Liao J 2011 arXiv:1101.0290 [nucl-th]
[31] Niemi H *et al* 2011 arXiv:1101.2442 [nucl-th]
[32] Huovinen P and Molnar D 2009 *Phys. Rev.* C **79** 014906 (arXiv:0808.0953 [nucl-th])
[33] Hidaka Y and Pisarski R D 2009 *Nucl. Phys.* A **820** 91C–4C (arXiv:0811.1202 [hep-ph])
[34] Meyer H B 2010 arXiv:1012.0234 [hep-lat]
[35] Alver B *et al* 2008 arXiv:0805.4411 [nucl-ex]
[36] Alver B *et al* 2008 *Phys. Rev.* C **77** 014906 (arXiv:0711.3724 [nucl-ex])
[37] Voloshin S A, Poskanzer A M, Tang A and Wang G 2008 *Phys. Lett.* B **659** 537 (arXiv:0708.0800 [nucl-th])
[38] Hirano T, Huovinen P and Nara Y 2010 arXiv:1012.3955 [nucl-th]
[39] Song H *et al* 2011 arXiv:1101.4638 [nucl-th]
[40] Andrade R, Grassi F, Hama Y, Kodama T and Socolowski O Jr 2006 *Phys. Rev. Lett.* **97** 202302
[41] Schenke B, Jeon S and Gale C 2010 arXiv:1009.3244 [hep-ph]
[42] Drescher H-J *et al* 2006 *Phys. Rev.* C **74** 044905 (arXiv:nucl-th/0605012)
[43] Albacete J L and Dumitru A 2010 arXiv:1011.5161 [hep-ph]
[44] Alt C *et al* [NA49 Collaboration] 2003 *Phys. Rev.* C **68** 034903 (arXiv:nucl-ex/0303001)
[45] Drescher H-J *et al* 2007 *Phys. Rev.* C **76** 024905 (arXiv:0704.3553 [nucl-th])
[46] Nagle J L, Steinberg P and Zajc W A 2010 *Phys. Rev.* C **81** 024901 (arXiv:0908.3684 [nucl-th])
[47] Masui H *et al* 2009 *Nucl. Phys.* A **830** 463C–6C (arXiv:0908.0403 [nucl-ex])